Journal of Lasers in Medical Sciences

J Lasers Med Sci 2023;14:e50

Original Article

http://journals.sbmu.ac.ir/jlms

doi 10.34172/jlms.2023.50

# Collagen Synthesis as a Prominent Process During the Interval between Two Laser Sessions

**Vahid Mansouri[1], Babak Arjmand[2,3], Maryam Hamzeloo-Moghadam[4], Mostafa Rezaei Tavirani[1*], Zahra Razzaghi[5], Alireza Ahmadzadeh[6], Mitra Rezaei[7,8], Reza M Robati[9]**

[1]Proteomics Research Center, Faculty of Paramedical Sciences, Shahid Beheshti University of Medical Sciences, Tehran, Iran
[2]Cell Therapy and Regenerative Medicine Research Center, Endocrinology and Metabolism Molecular-Cellular Sciences Institute, Tehran University of Medical Sciences, Tehran, Iran
[3]Iranian Cancer Control Center (MACSA), Tehran, Iran
[4]Traditional Medicine and Materia Medica Research Center, School of Traditional Medicine Shahid, Beheshti University of Medical Sciences, Tehran, Iran
[5]Laser Application in Medical Sciences Research Center, Shahid Beheshti University of Medical Sciences, Tehran, Iran
[6]Faculty of Paramedical Sciences, Shahid Beheshti University of Medical Sciences, Tehran, Iran
[7]Genomic Research Center, Shahid Beheshti University of Medical Sciences, Tehran, Iran
[8]Clinical Tuberculosis and Epidemiology Research Center, National Research Institute of Tuberculosis and Lung Diseases (NRITLD), Shahid Beheshti University of Medical Sciences, Tehran, Iran
[9]Skin Research Center, Shahid Beheshti University of Medical Sciences, Tehran, Iran

***Correspondence to**
Mostafa Rezaei Tavirani,
Email: tavirany@yahoo.com

**Received:** July 15, 2023
**Accepted:** September 4, 2023
**Published online:** October 28, 2023

**Abstract**

**Introduction:** Many people suffer from skin photodamage, especially photoaging. The application of a laser to repair damages is a common therapeutic method that is used widely. In the present study, the effectiveness and molecular mechanism of an Er:Glass non-ablative fractional laser on the human skin was assessed via bioinformatics and network analysis.

**Methods:** The gene expression profiles of 17 white female forearm skins which received an Er:Glass non-ablative fractional laser before and after laser treatment in two sessions were extracted from Gene Expression Omnibus (GEO). Data were evaluated via GEO2R and the significant differentially expressed genes (DEGs) were assessed via protein-protein interaction (PPI) network analysis. The central nodes were identified and discussed for the compared set of samples.

**Results:** Five classes of samples were clustered in two categories: first, baseline, 7 and 14 days after the first session of laser treatment, and second, one day after the first laser session, 29 days after the first laser session, and 1 day after the second laser session. The gross cell functions such as cell division and cell cycle and immune response were highlighted as the early affected targets of the laser. Collagen synthesis was resulted after the first laser session.

**Conclusion:** In conclusion, the time interval between laser sessions plays a critical role in the effectiveness of laser therapy. Findings indicate that the gross effect of laser application appears in a short time, and important processes such as collagen synthesis happen later.

**Keywords:** Skin; Photoaging; Laser; Collagen; Human.

## Introduction

Many people are exposed to sunlight and suffer from photodamage. The signs of skin photoaging that have been known for many years are lentigines, rhytids, keratoses, loss of elasticity, loss of translucency, telangiectasia, and sallow color.[1] Many documents about skin aging point out the thinning of skin due to epidermal cell layer atrophy and the decrease of fibroblasts and extracellular matrix components in dermal layers. Fragmentation and decrease of collagen are the two reported processes.[2]

Laser as a therapeutic method is used widely in dermatology. The application of fractional laser resurfacing in the treatment of photoaging via the promotion of neocollagenesis is an efficient method in clinics.[3] However, there are other methods such as laser-assisted nanoparticle delivery which can improve the skin health of the photoaged individuals.[4] Kim et al published a document about the improvement of photoaging-associated facial hyperpigmentation by using a picosecond 1064-nm neodymium-doped yttrium aluminum garnet laser.[5] There are pieces of evidence that laser treatment is accompanied by the alteration of many

**Please cite this article as follows:** Mansouri V, Arjmand B, Hamzeloo-Moghadam M, Rezaei Tavirani M, Razzaghi Z, Ahmadzadeh A, et al. Collagen synthesis as a prominent process during the interval between two laser sessions. *J Lasers Med Sci.* 2023;14:e50. doi:10.34172/jlms.2023.50.

gene expressions. On the basis of Garza and colleagues' report, due to the application of the laser, a robust gene expression signature relative to immune response and double-stranded RNA signaling appeared in the treated participants.[6]

Genomics methods such as microarrays, which investigate gene expression alterations, provide a large number of dysregulated genes under the applied condition.[7] There are several microarray experiments relative to laser effects on the skin.[8] Due to the large size of the microarray, bioinformatics is suitable for the assessment of the finding of the microarray. In such evaluation, data clustering, data screening, and network analysis are useful tools to reduce the dimension of data and provide an informative concept.[9,10] In such an investigation, a few numbers of main targeted genes are identified as central genes and the affected biological processes are determined [11]. In the present investigation, the gene expression profiles of 17 participants who were suffering from photoaging were extracted from GEO to be evaluated via bioinformatic tools. The samples were prepared before laser treatment and 1, 7, 14, and 29 days after laser application. The last individual received the second laser 28 days after the first laser treatment. It was expected that the importance of the time interval between two sessions of laser radiation would be validated by data analysis.

## Methods

GEO as a source of data was searched for the effects of the Er:Glass non-ablative fractional laser on the human skin. 119 samples (GSM6255319-GSM6255437) belonging to the gene expression profiles of forearm skins of 17 white females were recorded in GSE206495. The females were characterized by moderate-sever photoaging damages. The samples were provided as baseline, 1, 7, and 14 days after receiving a 1550 nm Er:Glass non-ablative fractional laser. The used laser setting was reported as fluence 60-70 mJ, treatment level 6-9, 8 passes (https://www.ncbi.nlm.nih.gov/geo/query/acc.cgi?acc = GSM6255319). More details of the methods are described in GSE206495 (https://www.ncbi.nlm.nih.gov/geo/query/acc.cgi?acc = gse206495). The additional profiles were provided for the 17 samples, 29 days after the first radiation and one day after the second laser session. To detect molecular events resulting from laser radiation, five comparative analyses of gene expression profiles including "one day after laser treatment" vs "baseline" (D1), "7 days after laser treatment" vs "baseline" (D7), "14 days after laser treatment" vs "baseline" (D14), "29 days and 1 day after the first and second laser sessions" vs "baseline" (D29), and "29 days and 1 day after the first and second laser sessions" vs "one day after laser treatment" (D29-1) were administrated.

The studied samples were analyzed based on box plots, expression density plots, adjusted P-value histograms, and uniform manifold approximation and projection (UMAP) plots by using the GEO2R program. In the next step, the top 250 differentially expressed genes (DEGs) (based on the smaller Padj value) were identified for each analysis. Considering Padj < 0.05, the significant DEGs were selected among the top 250 DEGs. The significant DEGs were imported in the "protein query" of the STRING database, and the recognized genes were included in a protein-protein interaction (PPI) network via Cytoscape software. To maximize interactions between the queried DEGs and the reduction of the isolated nodes, optimum numbers of the first neighbor genes from the STRING database were added to the queried DEGs.

The constructed PPI networks were analyzed via the "Network Analyzer" application of Cytoscape. The top 10% of nodes based on degree value, betweenness centrality, closeness centrality, and stress were identified as the central nodes of the studied networks. The common central nodes were selected as the potent hub-bottleneck nodes for each analysis.

## Results

The gene expression profiles were assessed via box plot analysis. Results indicated that all plots were characterized by similar medians and patterns of distribution (see Figure 1). Similar to box plots, a comparable pattern appeared in the expression density plot. The expression plots of 119 samples which were grouped into five classes are shown in Figure 2. The significant DEGs which discriminated the analyzed groups were determined via the GEO2R program. As shown in Table 1, there is a large number of significant DEGs for analyses on D1 and D29, while minimum numbers are related to the D29-1 analysis. The assessment of group similarity via UMAP evaluation provided a comprehensive understanding of the relationship between the studied groups. As depicted in Figure 3, five classes of the sample are grouped into 2 clusters including "one day after laser treatment" (1D) and "29 days and 1 day after the first and second laser sessions" (29D) as class-1 and "Baseline" (B), "7 days after laser treatment" (7D), and "14 days after laser treatment" (14D), as class-2. Diagrams of P-adj counts which visualize the relationship between the number of probes and $P_{adj}$ were provided for the five administrated evaluations (see Figure 4). The distribution of quantities based on P-adjusted is shown in Figure 4. A large number of DEGs are characterized by a $P$ value < 0.05 for the samples of 1D and 29D.

Among the 250 selected DEGs for D1 analysis, 181 individuals were recognized by the STRING database. The PPI network was constructed by the 181 DEGs plus added 100 first neighbors. The network including 27 isolated genes, 2 paired DEGs, and a main connected component of 252 nodes was formed by Cytoscape software. The potent

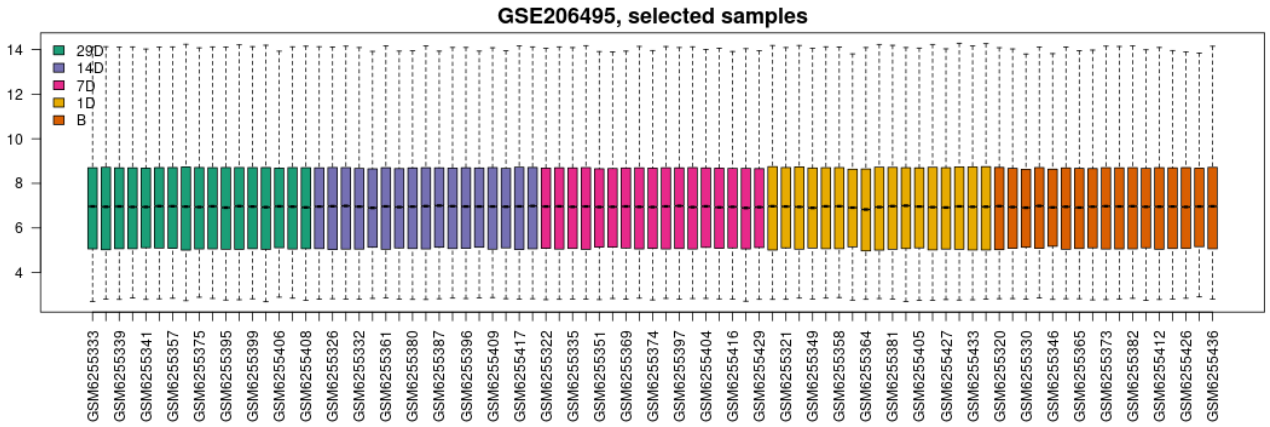


**Figure 1**. Box plots of the 119 Analyzed Samples of the CATEGORIZED FIVE GROUPS. The abbreviations are as follows: B; baseline, 1D; 1 day after laser treatment, 7D; 7 days after laser treatment, 14D; 14 days after laser treatment, and 29D; 29 days and 1 day after the first and second laser sessions respectively

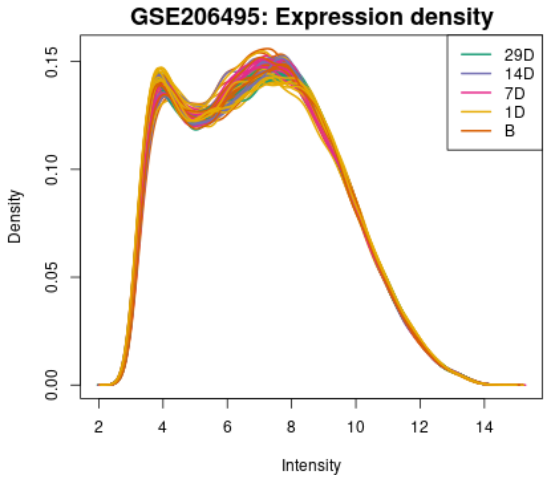


**Figure 2**. Expression Density Plot of the 119 Evaluated Samples Assembled Into Five Courses. The abbreviations are as follows: B; baseline, 1D; 1 day after laser treatment, 7D; 7 days after laser treatment, 14D; 14 days after laser treatment, and 29D; 29 days and 1 day after the first and second laser sessions

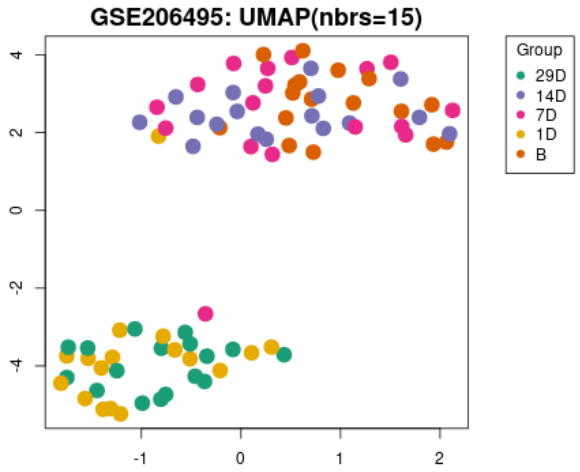


**Figure 3**. UMAP Clustering of Five Groups of Samples. The abbreviations are as follows: B; baseline, 1D; 1 day after laser treatment, 7D; 7 days after laser treatment, 14D; 14 days after laser treatment, and 29D; 29 days and 1 day after the first and second laser sessions

**Table 1**. Numbers of Significant DEGs Which Discriminate the Compared Groups (P-adj < 0.05)

| R | Type of Analysis | No. of Significant DEGs |
|---|---|---|
| 1 | D1 | 19567 |
| 2 | D7 | 1453 |
| 3 | D14 | 395 |
| 4 | D29 | 20852 |
| 5 | D29-1 | 151 |

hub-bottlenecks of analysis are shown in Table 2. As with the D1 analysis, the PPI network of the D29 assessment was formed from 163 recognized DEGs plus added 100 first neighbors. The network including 11 isolated genes and a main connected component of 252 nodes was yielded. The 7 identified potent hub-bottleneck nodes of D29 analysis are shown in Table 2.

The PPI networks of D7 and D14 evaluations were constructed by (168 recognized DEGs + 100 added first neighbors) and (136 recognized DEGs + 100 added first neighbors) respectively. The networks include (26 isolated genes, 2 paired DEGs, and a main connected component of 240 nodes) and (12 isolated genes and a main connected component of 224 nodes) for D7 and D14 respectively. The related potent hub-bottlenecks of this analysis are presented in Table 2. Since maximum common hub-bottlenecks appeared for D7 and D14 analyses, the common nodes are shown via the Venn diagram in Figure 5.

There were 151 significant DEGs for D29-1 analysis and 76 individuals were recognized by the STRING database. The PPI network including three isolated DEGs and a main connected component of 173 nodes was constructed by 76 DEGs plus added 100 first neighbors. The four potent hub-bottlenecks of this analysis are shown in Table 2. Since this analysis contains significant points, the network without the added first neighbors including 10 sub-networks of 12 isolated DEGs, a sub-network of 10 nodes, and a main connected component of 54 nodes was formed and analyzed (see Figure 6).

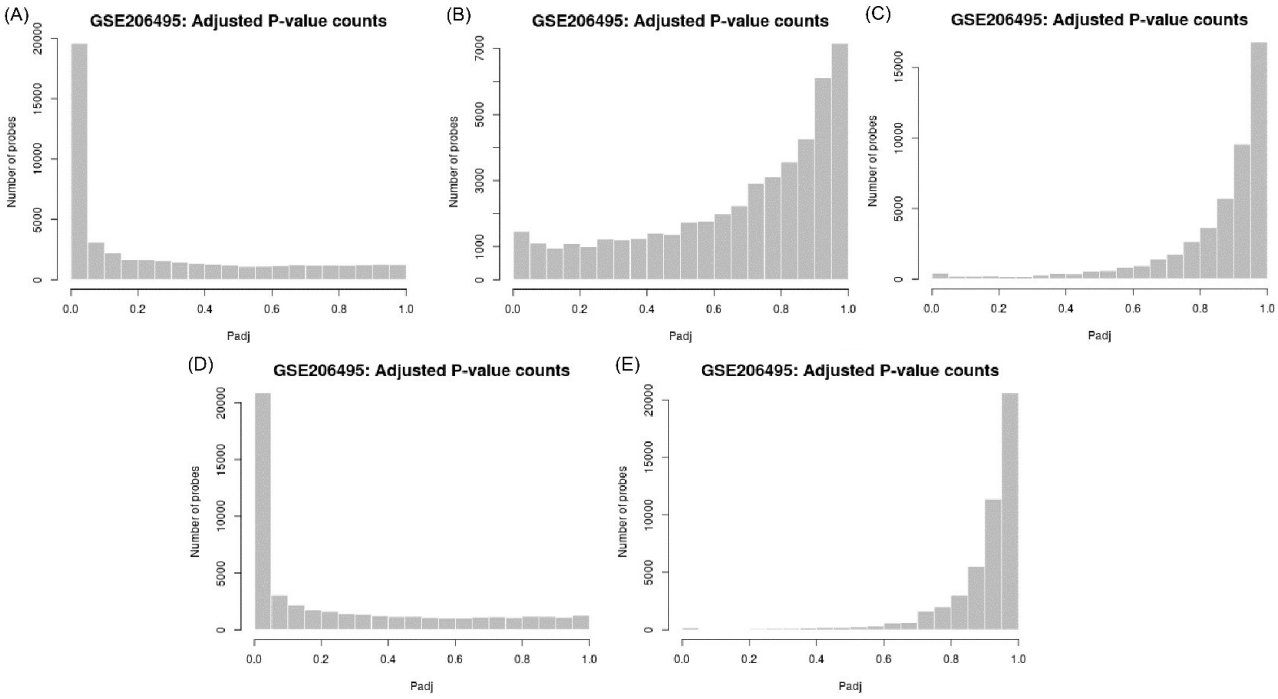


**Figure 4**. P-adj Count Histograms of (A) 1 Day After Laser Treatment vs Baseline, (B) 7 Days After Laser Treatment vs Baseline, (C)14 Days After Laser Treatment vs Baseline, (D) 29 Days and 1 Day After the First and Second Laser Sessions vs Baseline, and (E) 29 Days and 1 Day After the First and Second Laser Sessions vs 1 Day After Laser Treatment Analyses

## Discussion

The gene expression profiles of 17 females were investigated in different situations. Box plot analysis was used to compare gene expression profiles in the previous evaluations.[12] As it is shown in Figure 1, all samples were characterized by a similar plot in the presented plot. This property of samples was confirmed via an expression density plot (see Figure 2). The overlapping of curves in Figure 2 indicates that all samples are comparable. The rate of significant DEGs relative to laser treatment for the studied periods of days is shown in Table 1. The effect of non-ablative lasers on gene expression change has been discussed in previous investigations.[13] In the present research, considerable numbers of significant DEGs were extracted from D1 and D29 analysis, which corresponded to the deep effect of the applied laser on the gene expression profiles of the samples. Results (see Table 2) indicated that the number of DEGs decreased to 7.5% and 2% after 7 and 14 days, respectively, following laser treatment. It seems laser effects are repaired by the body. Sherrill et al published a document about dramatic changes in the gene expression of human skin one day after the administration of fractional laser. It is shown that alterations remain even after one month.[14] As it is depicted in Table 1, D29-1 is characterized by a minimum amount of DEGs. It can be concluded that the molecular events one day after laser treatment (for the first and the second sessions) are approximately similar.

UMAP analysis that is used frequently in the interpretation of genomic findings[15,16] indicates that 1D and 29D are separated from B, 7D, and 14D groups (see Figure 3). This finding refers to the considerable fast response of the body to laser treatment. The presence of D7 and D14 beside the B group corresponds to the moderate gene expression changes after 7 and 17 days of laser application. The distribution of DEGs based on Padj (Figure 4) indicates that most of the DEGs of D1 and D29 analysis are characterized by Padj < 0.05. This finding confirms the results of Table 1.

The hub-bottleneck nodes, which were characterized by high values of closeness centrality and stress, were selected as potent hub-bottlenecks for each analysis. As shown in Table 2, D7 and D14 have the most common potent hub-bottleneck nodes (see Figure 5). 75% of the potent hub-bottlenecks of D7 and 60% of the central nodes of D14 are common. On the other hand, NPM1 is a single common potent hub-bottleneck between D1 and D29 analyses. The significant roles of hub-bottlenecks in the control of biological processes have been highlighted in many researches.[17,18]

Analysis of D29-1 (see Figure 6) revealed a precious point about the difference between the function of the skin in "1 day after the first laser treatment" and "29 days and 1 day after the first and second laser sessions".

A sub-network of 10 nodes including COL1A1, COL1A2, COL3A1, COL5A1, COL5A2, COL6A1, INHBA, SPARC, POSTN, and FNDC1 appeared as a unit of DEGs which discriminate the two positions. It can be concluded that there are similarities accompanied by important differences between the gene expression

**Table 2.** The potent hub-bottleneck nodes of the five analyses.

| Type of Analysis | R | Display Name | Degree | Betweenness Centrality | Closeness Centrality | Stress |
|---|---|---|---|---|---|---|
| D1 | 1 | RUVBL1 | 96 | 0.012 | 0.557 | 14246 |
| | 2 | NPM1 | 95 | 0.011 | 0.582 | 18824 |
| | 3 | RPL35A | 82 | 0.013 | 0.510 | 15048 |
| D29 | 1 | ACTB | 110 | 0.050 | 0.624 | 66232 |
| | 2 | ISG15 | 93 | 0.040 | 0.581 | 59010 |
| | 3 | NPM1 | 73 | 0.016 | 0.558 | 21086 |
| | 4 | OASL | 70 | 0.017 | 0.518 | 33878 |
| | 5 | SEC61A1 | 70 | 0.011 | 0.539 | 13246 |
| | 6 | HSPA5 | 67 | 0.019 | 0.558 | 24052 |
| | 7 | ENO1 | 59 | 0.012 | 0.544 | 13828 |
| D7 | 1 | STAT1 | 149 | 0.041 | 0.699 | 55796 |
| | 2 | IRF7 | 128 | 0.018 | 0.634 | 34334 |
| | 3 | MX1 | 124 | 0.015 | 0.616 | 31708 |
| | 4 | ISG15 | 120 | 0.034 | 0.636 | 38666 |
| | 5 | DDX58 | 119 | 0.018 | 0.622 | 36340 |
| | 6 | IFIH1 | 115 | 0.014 | 0.602 | 32614 |
| | 7 | IRF8 | 101 | 0.009 | 0.587 | 20722 |
| | 8 | RSAD2 | 101 | 0.009 | 0.569 | 13648 |
| D14 | 1 | STAT1 | 141 | 0.037 | 0.722 | 56342 |
| | 2 | CD4 | 134 | 0.024 | 0.715 | 38702 |
| | 3 | IRF8 | 123 | 0.029 | 0.676 | 40846 |
| | 4 | PTPRC | 121 | 0.020 | 0.682 | 27310 |
| | 5 | CD86 | 119 | 0.011 | 0.678 | 22580 |
| | 6 | IRF7 | 119 | 0.015 | 0.662 | 31124 |
| | 7 | MX1 | 113 | 0.013 | 0.644 | 30302 |
| | 8 | TLR7 | 110 | 0.020 | 0.656 | 27078 |
| | 9 | DDX58 | 107 | 0.016 | 0.637 | 32690 |
| | 10 | IFIH1 | 107 | 0.020 | 0.635 | 33230 |
| D29-1 | 1 | STAT1 | 139 | 0.037 | 0.837 | 23512 |
| | 2 | IRF7 | 131 | 0.028 | 0.798 | 20952 |
| | 3 | MX1 | 127 | 0.023 | 0.773 | 18248 |
| | 4 | ISG15 | 123 | 0.017 | 0.759 | 15600 |

profiles of D1 and D29. Narda et al published a document about a mechanism in which glycolic acid can reverse skin age and photodamages. Based on this report, glycolic acid can increase skin collagen levels significantly.[19] It can be concluded that with glycolic acid, the first laser radiation has affected the collagen production of the skin, and the irritated skin in the second laser session has different levels of collagen relative to the skin of the 1D group. The findings refer to the administration of repetitive laser administration to achieve effective treatment.

STAT1, IRF7, MX1, DDX58, IFIH1, and IRF8 are the six common potent hub-bottlenecks between D7 and D14 analyses.

Interferon-regulatory factors (IRFs) which are intracellular proteins play a role in the regulation of

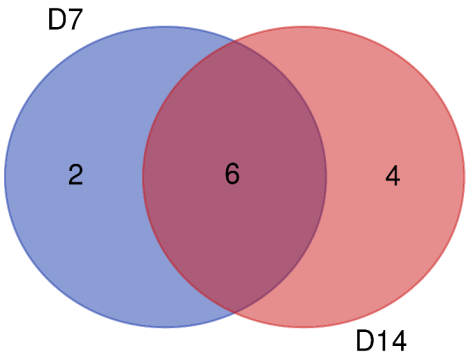


**Figure 5.** Venn Diagram of Potent Hub-Bottleneck Nodes of D7 and D14 Analysis

immune cell maturation.[20] Based on the report of Kong et al, STAT1, MX1, DDX58, and IFIH1 appear as hub genes in systemic lupus erythematosus. Immunological responses of STAT1, MX1, DDX58, and IFIH1 are highlighted in this investigation.[21] It seems that the regulation of the immune system is the main function which happens in the skin during days between two sessions of laser application.

Nucleophosmin (NPM1) is the single common central node between D1 and D29 analyses. Several important roles such as chromatin remodeling, biogenesis of ribosome, DNA repair, DNA transcription, replication, and mitotic spindle formation are reported as functions of NPM1.[22] The prominent roles of NPM1 correspond to the deep effects of a laser on cell function and proliferation. Based on this statement, it can be expected that ACTB, ISG15, OASL, and SEC61A1 which appear as central genes in D29 analysis play critical roles in mitosis and cell division processes. As it is reported, Beta-actin (ACTB) is involved in several important cellular functions such as cell division, cell migration, wound healing, embryonic development, and immune response.[23] The key role of ISG15 in cell cycle progression is highlighted in the previous investigations.[24] Oligoadenylate synthase-like (OASL) is a member of the OSA family, which is involved in the degradation of cellular and viral RNA.[25] There are documents about the role of SEC61A1 in cell differentiation. Schubert and colleagues' investigation revealed that spliced X-box binding protein 1 targets SEC61A1 to induce plasma cell differentiation.[26]

## Conclusion

In conclusion, two main responses to laser application are seen in the skin. First, an early gross functional changes such as; cell division and cell cycle and the second response mostly via the immune system. Another important point refers to the interval days between two sequential laser radiations. It seems the optimal interval time can lead to more efficient treatment. Collagen production was highlighted as a significant activity in the interval time between two laser sessions. Due to the gross

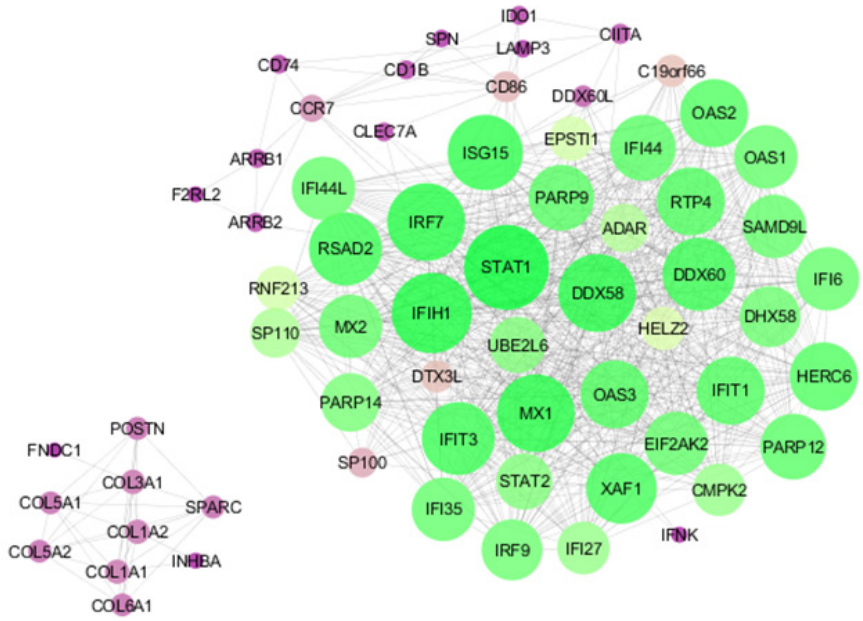


**Figure 6.** Two Subnetworks of the PPI Network of D29-1 Analysis. The 12 isolated DEGs are not shown. Nodes are visualized based on degree value. The bigger size of nodes and green color refer to a larger value of degree

effects of laser treatment on fundamental cell functions such as proliferation, cell cycle, and mitotic processes, it can be recommended that the probable side effects should be studied in future investigations. Following the samples up for a couple of years can provide useful information.


## Acknowledgments

This project was supported by Shahid Beheshti University of Medical Sciences.


## Authors' Contribution

**Conceptualization:** Vahid Mansouri, Mostafa Rezaei Tavirani, Reza M Robati.
**Data curation:** Zahra Razzaghi, Alireza Ahmadzadeh.
**Formal analysis:** Mitra Rezaei.
**Funding acquisition:** Vahid Mansouri.
**Investigation:** Maryam Hamzeloo-Moghadam.
**Methodology:** Zahra Razzaghi.
**Project administration:** Babak Arjmand, Maryam Hamzeloo-Moghadam.
**Resources:** Alireza Ahmadzadeh.
**Software:** Zahra Razzaghi.
**Supervision:** Reza M Robati, Mostafa Rezaei Tavirani, Mitra Rezaei.
**Validation:** Babak Arjmand.
Visualization: Zahra Razzaghi.
**Writing–original draft:** Vahid Mansouri, Mostafa Rezaei Tavirani.
**Writing–review editing:** Babak Arjmand, Maryam Hamzeloo-Moghadam, Mostafa Rezaei Tavirani, Zahra Razzaghi, Alireza Ahmadzadeh, Mitra Rezaei, Reza M Robati.

## Competing Interests

The authors declare that they have no conflict of interest.

## Ethical Approval

This project was approved by the ethical committee of Shahid Beheshti University of Medical Sciences (code: IR.SBMU.LASER.REC.1402.011).

## References


1. Glogau RG. Aesthetic and anatomic analysis of the aging skin. Semin Cutan Med Surg. 1996;15(3):134-8. doi: 10.1016/s1085-5629(96)80003-4.
2. Salminen A, Kaarniranta K, Kauppinen A. Photoaging: UV radiation-induced inflammation and immunosuppression accelerate the aging process in the skin. Inflamm Res. 2022;71(7-8):817-31. doi: 10.1007/s00011-022-01598-8.
3. Borges J, Araújo L, Cuzzi T, Martinez L, Gonzales Y, Manela-Azulay M. Fractional laser resurfacing treats photoaging by promoting neocollegenesis and cutaneous edema. J Clin Aesthet Dermatol. 2020;13(1):22-7.
4. Lee WR, Huang TH, Hu S, Alalaiwe A, Wang PW, Lo PC, et al. Laser-assisted nanoparticle delivery to promote skin absorption and penetration depth of retinoic acid with the aim for treating photoaging. Int J Pharm. 2022;627:122162. doi: 10.1016/j.ijpharm.2022.122162.
5. Kim YJ, Suh HY, Choi ME, Jung CJ, Chang SE. Clinical improvement of photoaging-associated facial hyperpigmentation in Korean skin with a picosecond 1064-nm neodymium-doped yttrium aluminum garnet laser. Lasers Med Sci. 2020;35(7):1599-606. doi: 10.1007/s10103-020-03008-z.
6. Garza LA, Sheu M, Kim N, Tsai J, Alessi Cesar SS, Lee J, et al. Association of early clinical response to laser rejuvenation of photoaged skin with increased lipid metabolism and restoration of skin barrier function. J Invest Dermatol. 2023;143(3):374-85.e7. doi: 10.1016/j.jid.2022.07.024.
7. Maniruzzaman M, Rahman MJ, Ahammed B, Abedin MM, Suri HS, Biswas M, et al. Statistical characterization and classification of colon microarray gene expression data using multiple machine learning paradigms. Comput Methods Programs Biomed. 2019;176:173-93. doi: 10.1016/j.cmpb.2019.04.008.
8. Huth S, Huth L, Marquardt Y, Cheremkhina M, Heise R, Baron JM. MMP-3 plays a major role in calcium pantothenate-promoted wound healing after fractional ablative laser treatment. Lasers Med Sci. 2022;37(2):887-94. doi: 10.1007/s10103-021-03328-8.

9. Suzuki A, Horie T, Numabe Y. Investigation of molecular biomarker candidates for diagnosis and prognosis of chronic periodontitis by bioinformatics analysis of pooled microarray gene expression datasets in Gene Expression Omnibus (GEO). BMC Oral Health. 2019;19(1):52. doi: 10.1186/s12903-019-0738-0.
10. Abbaszadeh HA, Peyvandi AA, Sadeghi Y, Safaei A, Zamanian-Azodi M, Khoramgah MS, et al. Er:YAG laser and cyclosporin A effect on cell cycle regulation of human gingival fibroblast cells. J Lasers Med Sci. 2017;8(3):143-9. doi: 10.15171/jlms.2017.26.
11. Zamanian-Azodi M, Rezaei-Tavirani M, Hasanzadeh H, Rahmati Rad S, Dalilan S. Introducing biomarker panel in esophageal, gastric, and colon cancers; a proteomic approach. Gastroenterol Hepatol Bed Bench. 2015;8(1):6-18.
12. Kohlmann A, Kipps TJ, Rassenti LZ, Downing JR, Shurtleff SA, Mills KI, et al. An international standardization programme towards the application of gene expression profiling in routine leukaemia diagnostics: the Microarray Innovations in LEukemia study prephase. Br J Haematol. 2008;142(5):802-7. doi: 10.1111/j.1365-2141.2008.07261.x.
13. Huth L, Huth S, Marquardt Y, Winterhalder P, Steiner T, Hölzle F, et al. Deciphering the molecular effects of non-ablative Er:YAG laser treatment in an in vitro model of the non-keratinized mucous membrane. Lasers Med Sci. 2021;36(5):1117-21. doi: 10.1007/s10103-020-03149-1.
14. Sherrill JD, Finlay D, Binder RL, Robinson MK, Wei X, Tiesman JP, et al. Transcriptomic analysis of human skin wound healing and rejuvenation following ablative fractional laser treatment. PLoS One. 2021;16(11):e0260095. doi: 10.1371/journal.pone.0260095.
15. Yang Y, Sun H, Zhang Y, Zhang T, Gong J, Wei Y, et al. Dimensionality reduction by UMAP reinforces sample heterogeneity analysis in bulk transcriptomic data. Cell Rep. 2021;36(4):109442. doi: 10.1016/j.celrep.2021.109442.
16. Diaz-Papkovich A, Anderson-Trocmé L, Ben-Eghan C, Gravel S. UMAP reveals cryptic population structure and phenotype heterogeneity in large genomic cohorts. PLoS Genet. 2019;15(11):e1008432. doi: 10.1371/journal.pgen.1008432.
17. Mateus Pellenz F, Crispim D, Silveira Assmann T. Systems biology approach identifies key genes and related pathways in childhood obesity. Gene. 2022;830:146512. doi: 10.1016/j.gene.2022.146512.
18. Karbalaei R, Allahyari M, Rezaei-Tavirani M, Asadzadeh-Aghdaei H, Zali MR. Protein-protein interaction analysis of Alzheimer`s disease and NAFLD based on systems biology methods unhide common ancestor pathways. Gastroenterol Hepatol Bed Bench. 2018;11(1):27-33.
19. Narda M, Trullas C, Brown A, Piquero-Casals J, Granger C, Fabbrocini G. Glycolic acid adjusted to pH 4 stimulates collagen production and epidermal renewal without affecting levels of proinflammatory TNF-alpha in human skin explants. J Cosmet Dermatol. 2021;20(2):513-21. doi: 10.1111/jocd.13570.
20. Günthner R, Anders HJ. Interferon-regulatory factors determine macrophage phenotype polarization. Mediators Inflamm. 2013;2013:731023. doi: 10.1155/2013/731023.
21. Kong J, Li L, Zhimin L, Yan J, Ji D, Chen Y, et al. Potential protein biomarkers for systemic lupus erythematosus determined by bioinformatics analysis. Comput Biol Chem. 2019;83:107135. doi: 10.1016/j.compbiolchem.2019.107135.
22. Lindström MS. NPM1/B23: a multifunctional chaperone in ribosome biogenesis and chromatin remodeling. Biochem Res Int. 2011;2011:195209. doi: 10.1155/2011/195209.
23. Guo C, Liu S, Wang J, Sun MZ, Greenaway FT. ACTB in cancer. Clin Chim Acta. 2013;417:39-44. doi: 10.1016/j.cca.2012.12.012.
24. Vuillier F, Li Z, Commere PH, Dynesen LT, Pellegrini S. USP18 and ISG15 coordinately impact on SKP2 and cell cycle progression. Sci Rep. 2019;9(1):4066. doi: 10.1038/s41598-019-39343-7.
25. Choi UY, Kang JS, Hwang YS, Kim YJ. Oligoadenylate synthase-like (OASL) proteins: dual functions and associations with diseases. Exp Mol Med. 2015;47(3):e144. doi: 10.1038/emm.2014.110.
26. Schubert D, Klein MC, Hassdenteufel S, Caballero-Oteyza A, Yang L, Proietti M, et al. Plasma cell deficiency in human subjects with heterozygous mutations in Sec61 translocon alpha 1 subunit (SEC61A1). J Allergy Clin Immunol. 2018;141(4):1427-38. doi: 10.1016/j.jaci.2017.06.042.